Comparison with Observations of EUV and X-Ray Emissions Calculated with Different Heating Models for Active Region 7986

Roberto Lionello, Jon A. Linker, Zoran Mikić[1],
and Yung Mok[2]

lionellor@saic.com, linkerj@saic.com, mikicz@saic.com, ymok@uci.edu

[1]SAIC/CESS
[2]University of California, Irvine

Introduction

- We have begun a comparison of the calculated emission with observations for first Whole Sun Month campaign (late August 1996).
- We have made both a global model of the corona and one of AR 7986. Here we describe this second, local model.
- We have used a 3D MHD code to compute the magnetic field configuration.
- Then we have calculated the thermal properties of the plasma using a 3D hydrodynamic algorithm.
- We have explored different heating parameters and models.
- Synthetic emission images in EUV and X-Rays have been compared quantitatively with the EIT and SXT observations.

Multispectral Emission

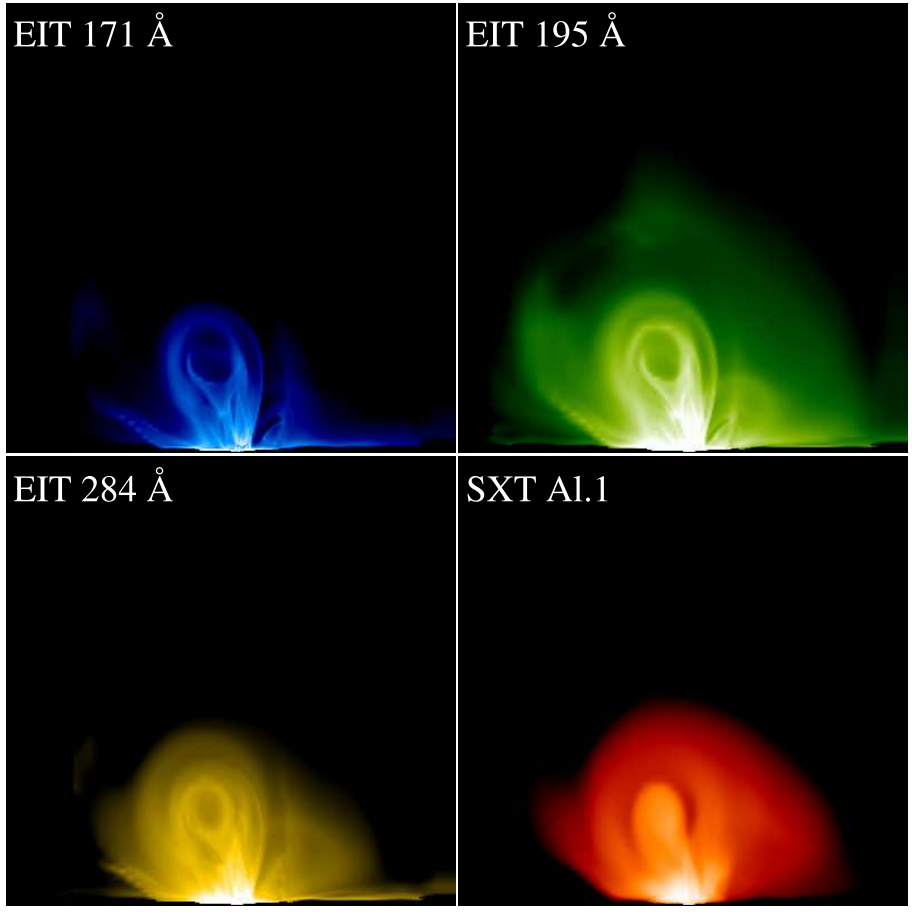

Calculated multispectral emission in EIT 171, 195, 284 Å and SXT Al.1, for AR7986 at the same instant in a 3D simulations. Our 3D MHD model can reproduce variations in emission in active regions in response to thermal instabilities, non-steady heating, and magnetic evolution.

Non Equilibrium Solutions

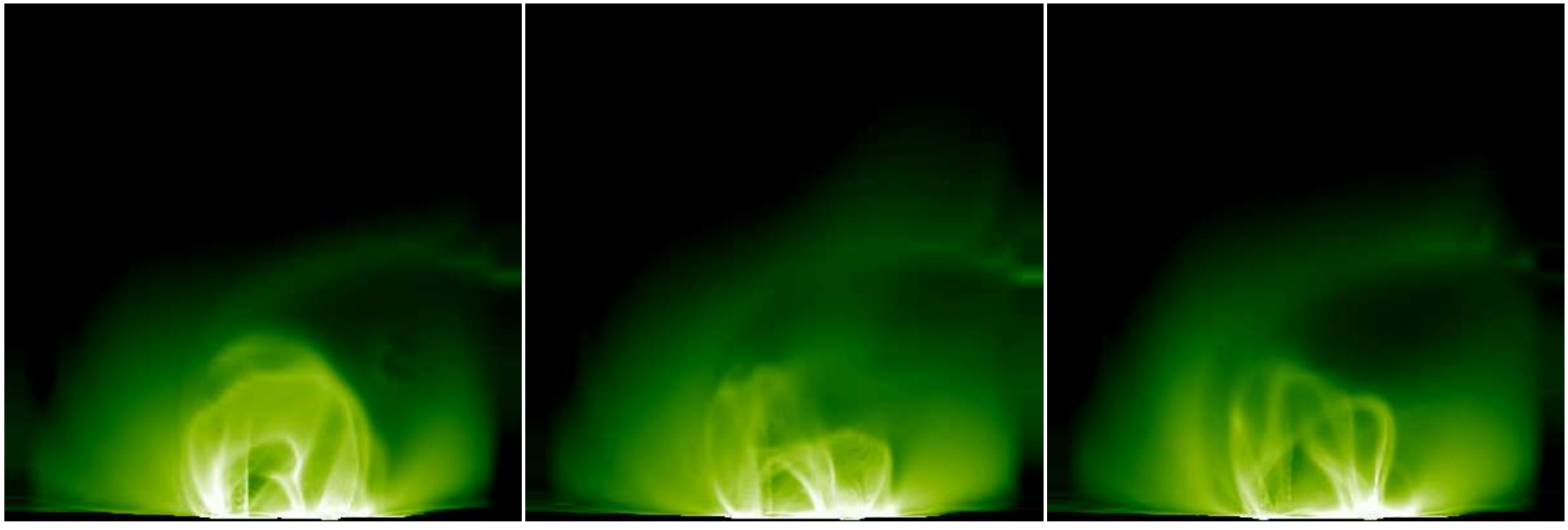

A sequence showing the evolution of the emission in the EIT 195 Å band. The magnetic field has been held fixed for this simulation and variations in emission are entirely due to thermal instabilities and/or nonequilibrium.

3D Plasma Model I

$$
\begin{aligned}
\frac{\partial \rho}{\partial t} + \nabla\cdot(v\hat{\mathbf{b}}\rho) &= 0, \\
\frac{1}{\gamma - 1}\left(\frac{\partial T}{\partial t} + v\hat{\mathbf{b}}\cdot\nabla T\right) &= -T\nabla\cdot v\hat{\mathbf{b}} + \frac{m}{k\rho}(\nabla\cdot\kappa\hat{\mathbf{b}}\hat{\mathbf{b}}\cdot\nabla T \\
&\quad -n_e n_p Q(T) + H_{\mathrm{ch}}), \\
\rho\left(\frac{\partial v}{\partial t} + v\hat{\mathbf{b}}\cdot\nabla v\right) &= \hat{\mathbf{b}}\cdot\left(-\nabla p + \rho\mathbf{g} + \nabla\cdot(\nu\rho\nabla v\hat{\mathbf{b}})\right).
\end{aligned}
$$

3D Plasma Model II

- We advance the 3D hydrodynamic equations along fixed magnetic field lines calculated with the 3D MHD model.
- The hydro model includes radiation losses, heating, and thermal conduction.
- Thermal conductivity κ and radiation loss function Q are modified to broaden the gradient in the transition region.
- Values of temperature ($20,000$ K) and density (2×10^{11} cm^{-3}) are fixed at the base of the domain.
- Heating model: $H_{\rm ch} = h_0 B^{\alpha} \rho^{\beta} + h_1 \exp\left(-z/\lambda\right)$

Impulsive Heating

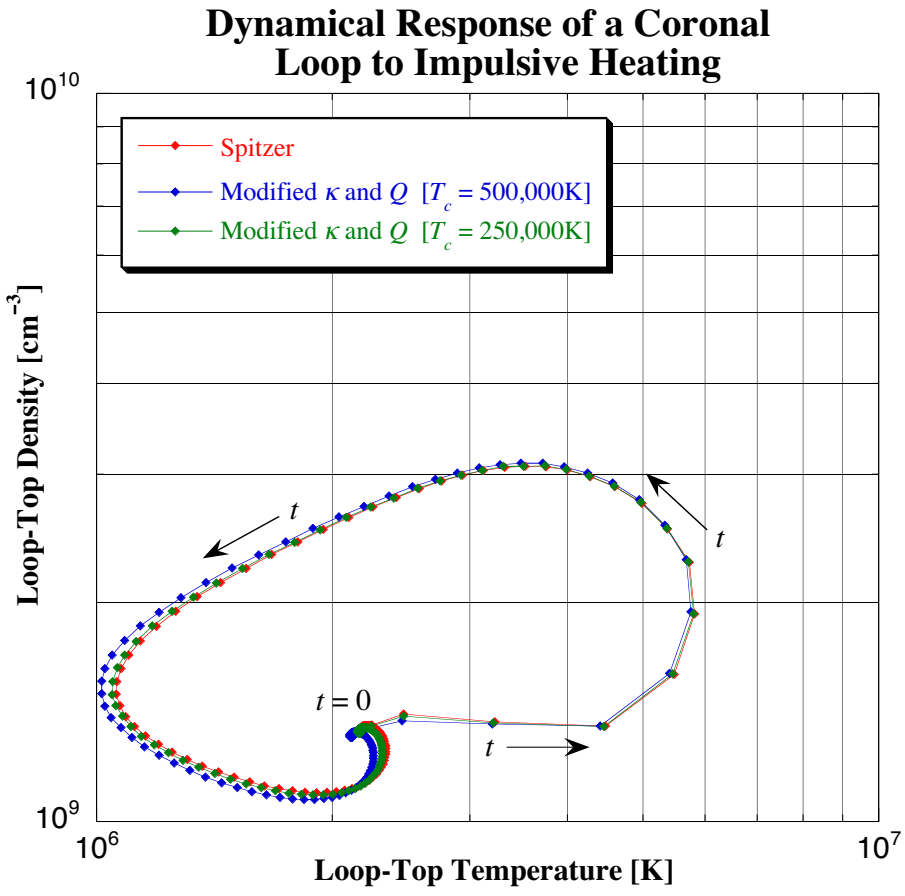

Evolution in the T-n plane of the top of a loop subject to a sudden heat pulse. The 1D computations were performed using our technique that broadens the transition region by modifying the Spitzer conductivity and radiation losses for $T < 250,000$ K or $T < 500,000$ K. The red curve uses the full Spitzer conductivity. Points are 145 s apart.

Synthetic Emission Images

- The flux of solar photons registered by an instrument in a given configuration i is given by

$$D = \int n_e^2(w) f_i(T(w), n_e(w))\, dw \quad [\mathrm{DN/s}] \ ,$$

  integrated along the line of sight w.
- $f_i(T, n_e)$ is a function that takes into account of atomic physics, geometry, and the properties of both the instrument and the filters.
- The $f_i(T, n_e)$s have weak dependency on n_e, which we neglected in this investigation.
- Given n_e and T from the simulations, synthetic images can be created and compared with the observations.

EIT and SXT Response Functions

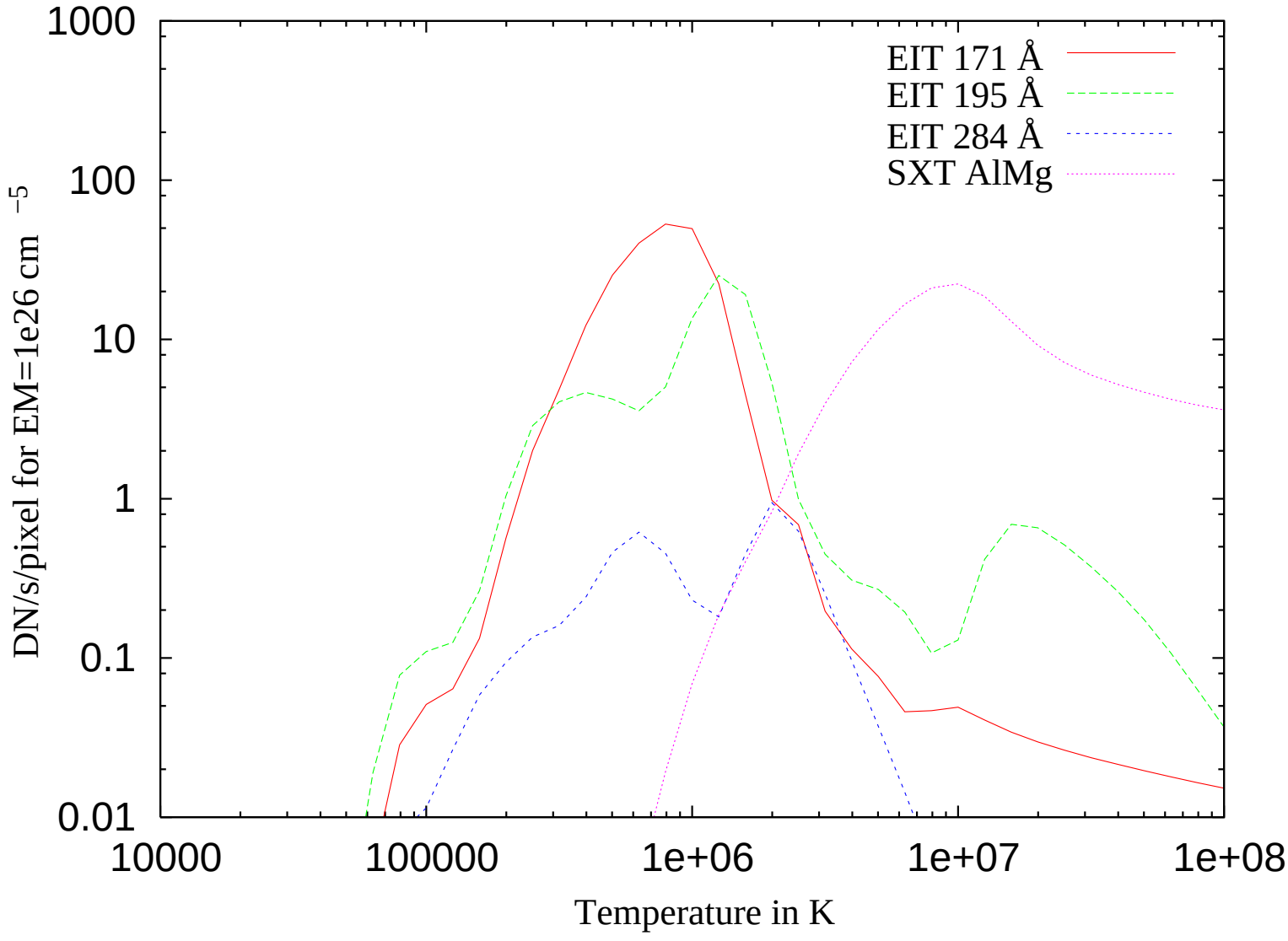

Models vs. Observations I

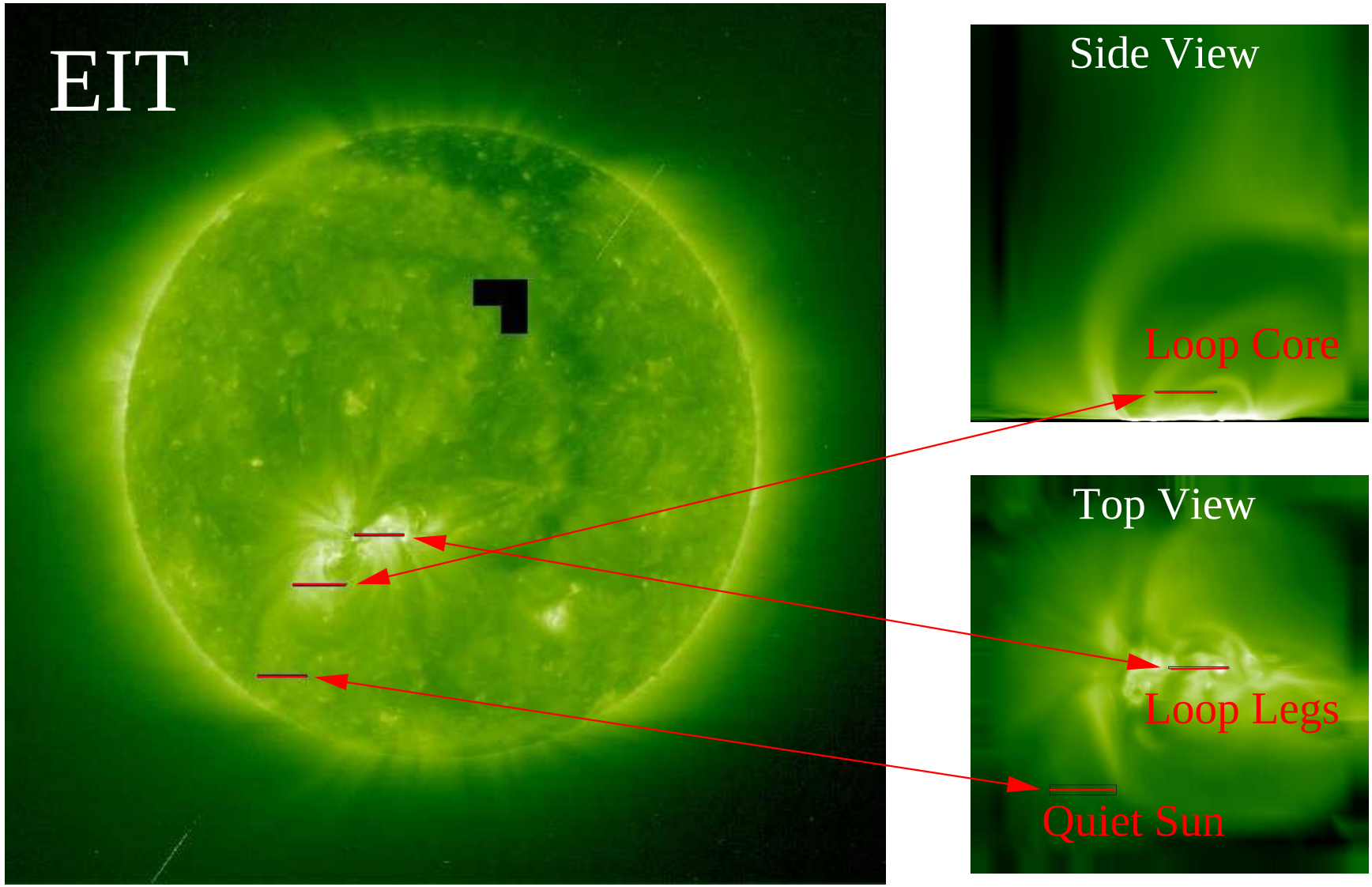

Models vs. Observations II

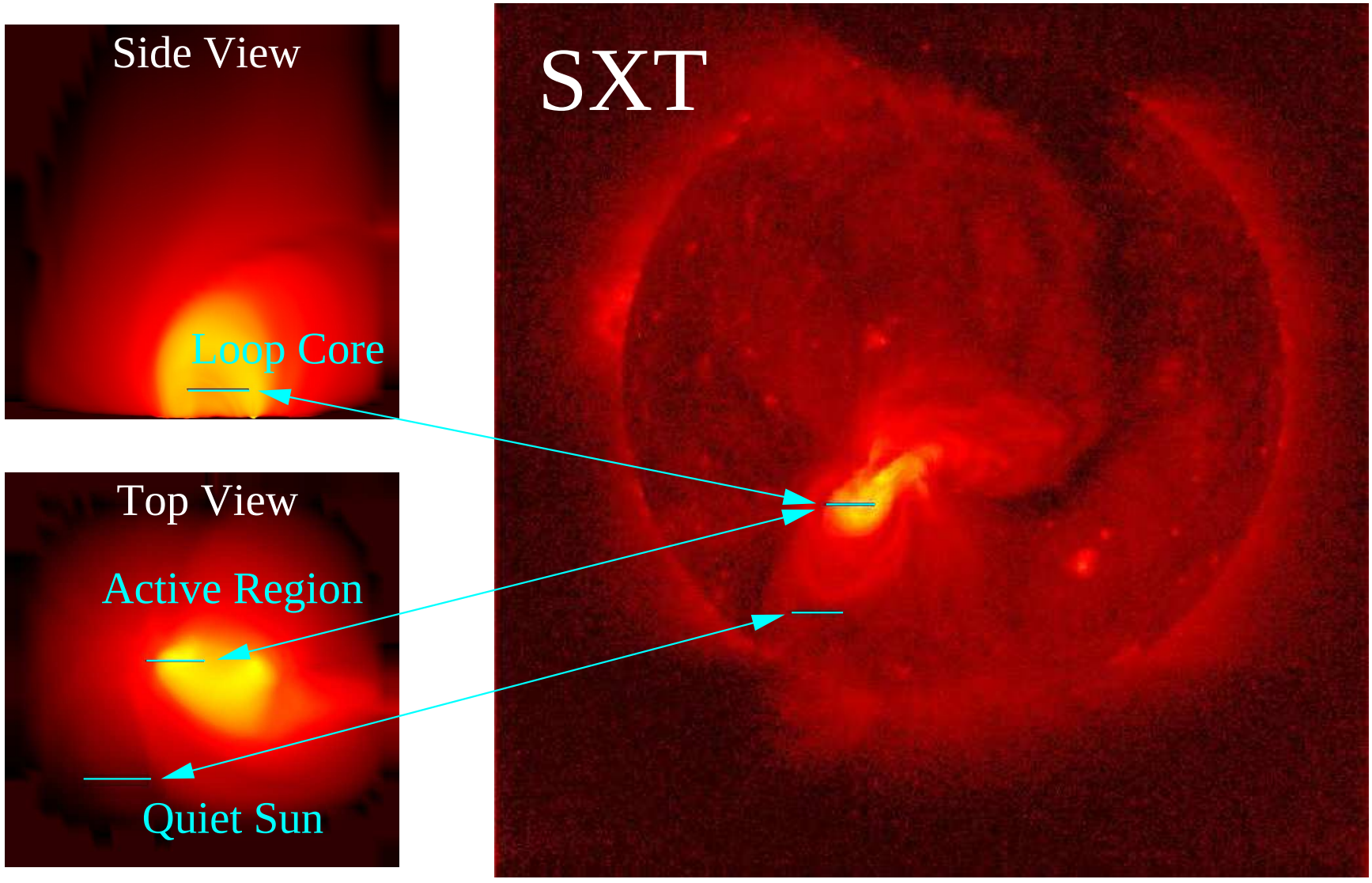

Models vs. Observations III

We have compared the observed emission at different points, chosen in locations shown in red for EIT or in cyan for SXT, with the values obtained with our models. In EIT (171, 195, and 284 Å), points are chosen in three locations and compared with the emission computed in the *xy* plane ("Loop Legs" and "Quiet Sun") and in the *xz* plane ("Loop Core"). "Loop Core" excludes EUV emission from the loop legs, which are rendered too bright in models. In SXT we have chosen two locations and compared them with the computed emission in the *xy* plane ("Quiet Sun" and "Active Region"). The same points compared with "Active Region" are compared with "Loop Core" in the *xz* plane because emission from cold loop legs is small in X-rays. These comparison are not meant to be point by point, but rather they provide an indicative range within which the time-dependent calculated emission should lie.

Case 940

- This is a case where we do not match observations, neither in the quiet Sun nor in the loop.
- The heating function is $H \propto B^3/\sqrt{\rho}$.
- Magnetic field configuration is a force-free field.

Case 940, $H \propto B^3/\sqrt{\rho}$: Top View

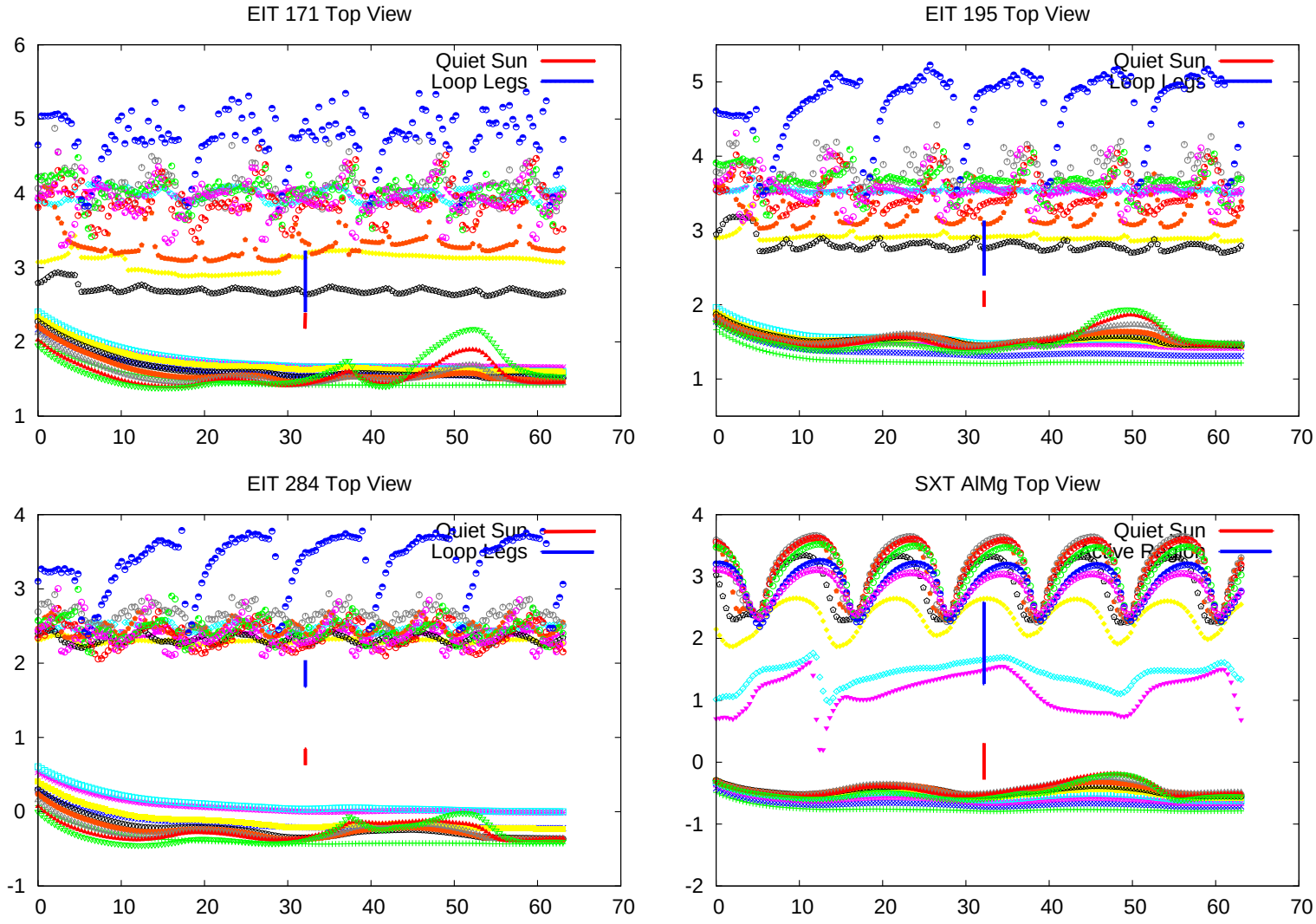

x axis: time in hours. y axis: emission in $\log 10\ DN/s/pixel$ (1024×1024 pixels).

Case 940, $H \propto B^3/\sqrt{\rho}$: Side View

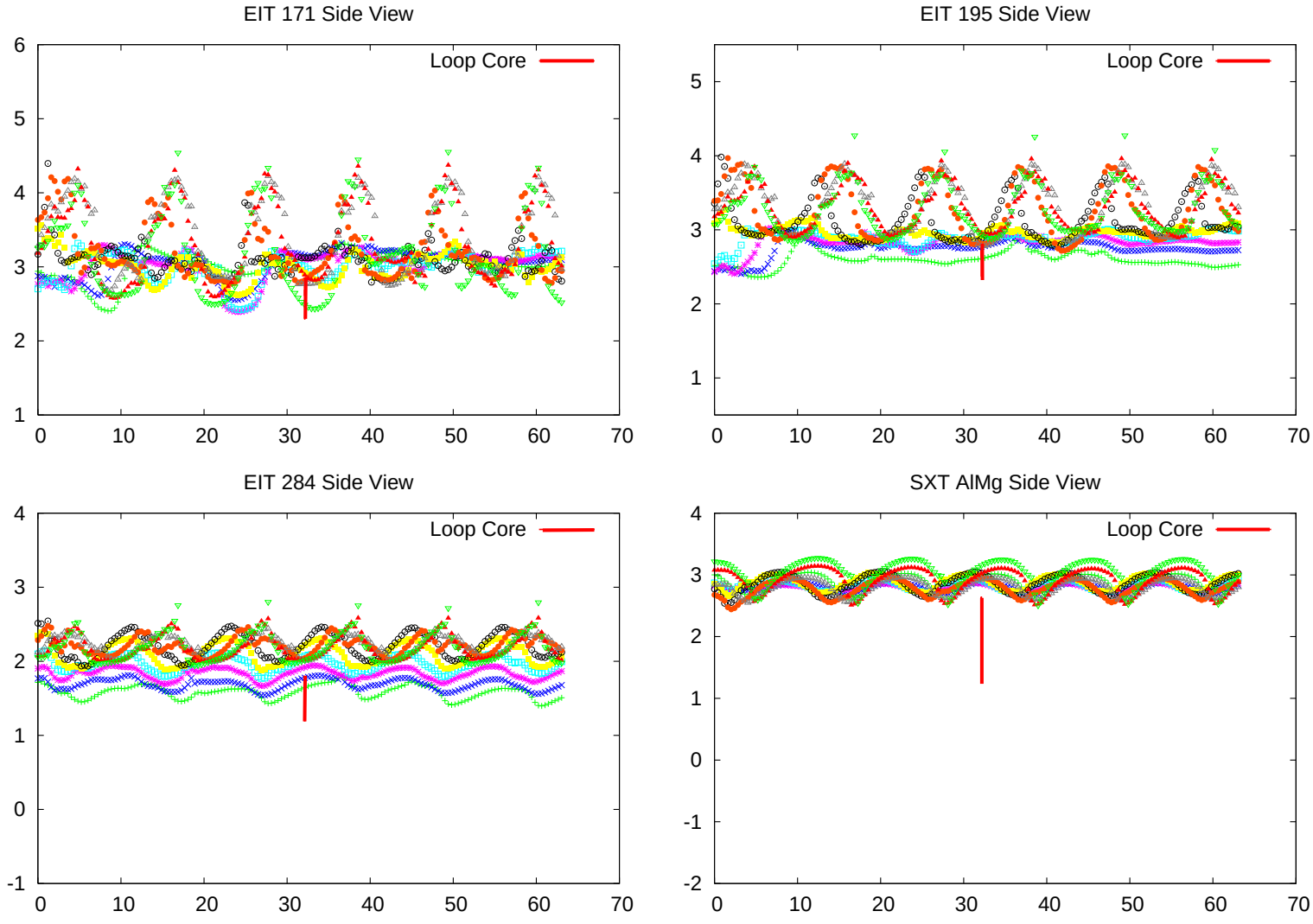

x axis: time in hours. y axis: emission in $\log 10\ DN/s/pixel$ (1024×1024 pixels).

Case 953

- In this case the calculated emission for the quiet Sun is closer to observations, but we obtain too much emission in the loop.
- The heating function is $H \propto B^{2.5}/\sqrt{\rho}$ and the heating was lifted by ten grid points. Heating constant was reduced twice at the beginning of the simulation
- Magnetic field configuration is the same as in the previous case.

Case 953, $H \propto B^{2.5}/\sqrt{\rho}$: Top View

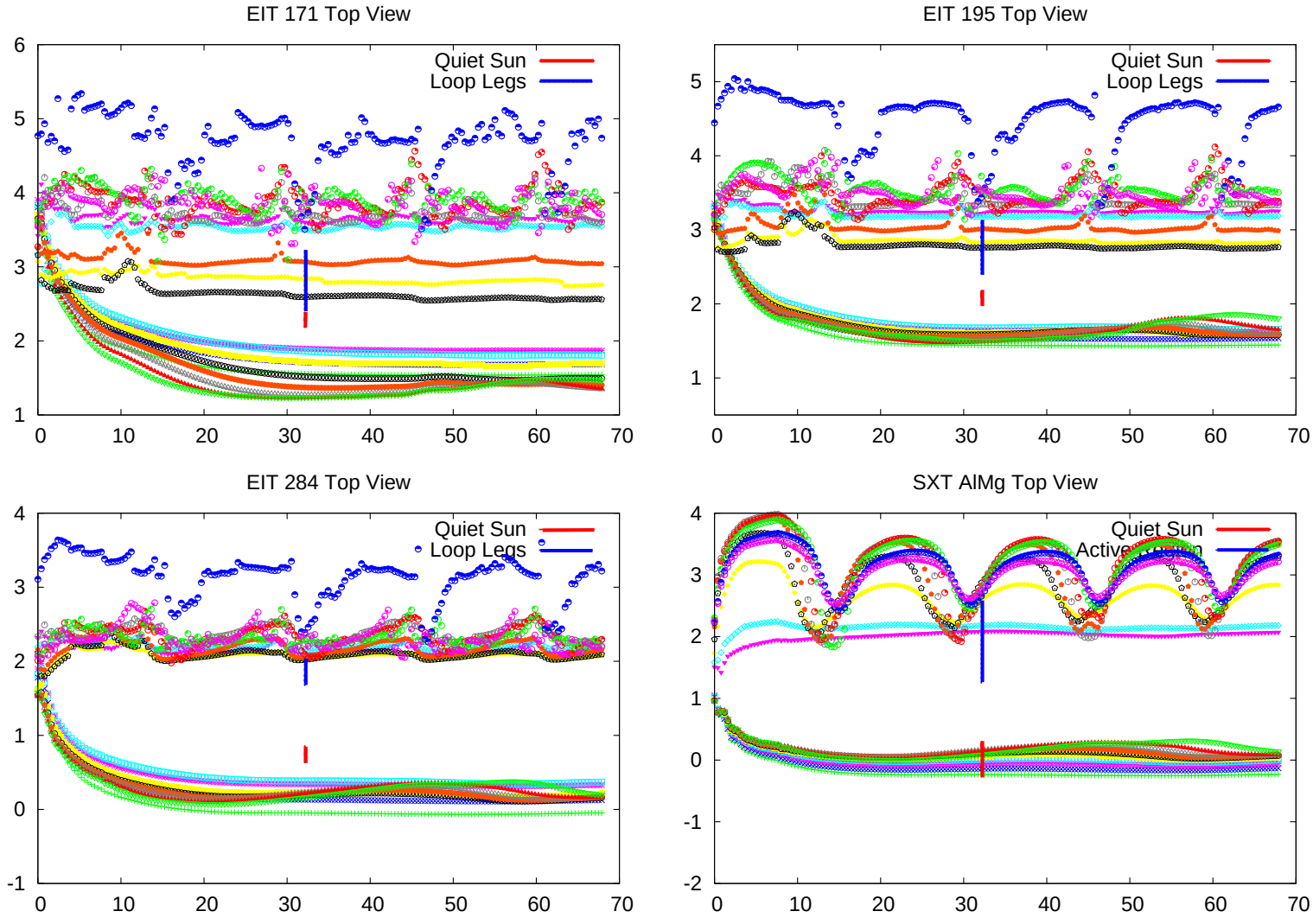

x axis: time in hours. y axis: emission in $\log 10\ DN/s/pixel$ (1024×1024 pixels).

Case 953, $H \propto B^{2.5}/\sqrt{\rho}$: Side View

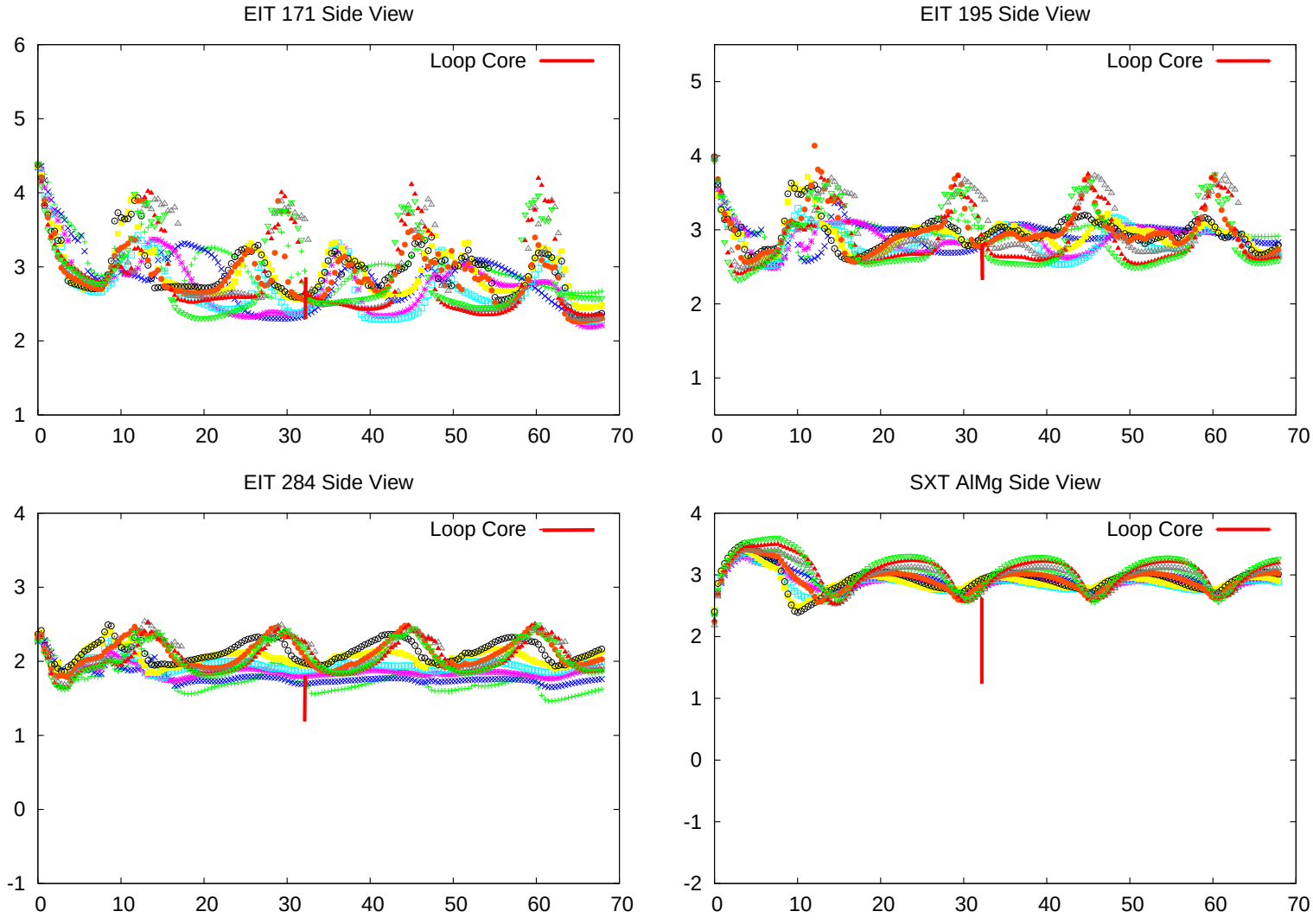

x axis: time in hours. y axis: emission in $\log 10\ DN/s/pixel$ (1024×1024 pixels).

Case 905

- This case has a better match in the loop core (especially for SXT) Calculated emission in the legs is still too high.
- The heating function is $H \propto B^3/\sqrt{\rho}$. The constant of proportionality varied.
- Magnetic field configuration is a force-free field.

Case 905, $H \propto B^3/\sqrt{\rho}$: Top View

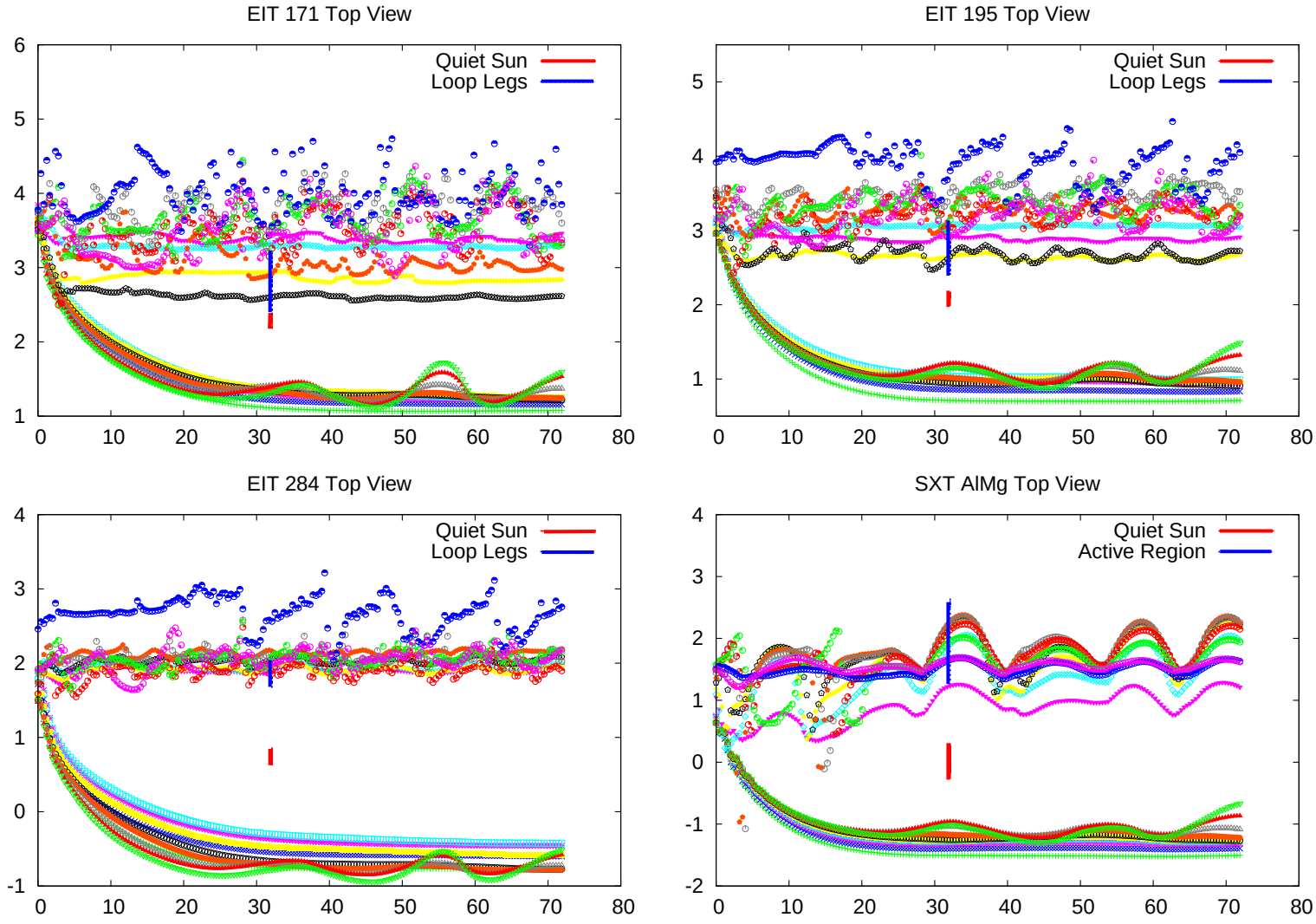

x axis: time in hours. y axis: emission in $\log 10\ DN/s/pixel$ (1024×1024 pixels).

Case 905, $H \propto B^3/\sqrt{\rho}$: Side View

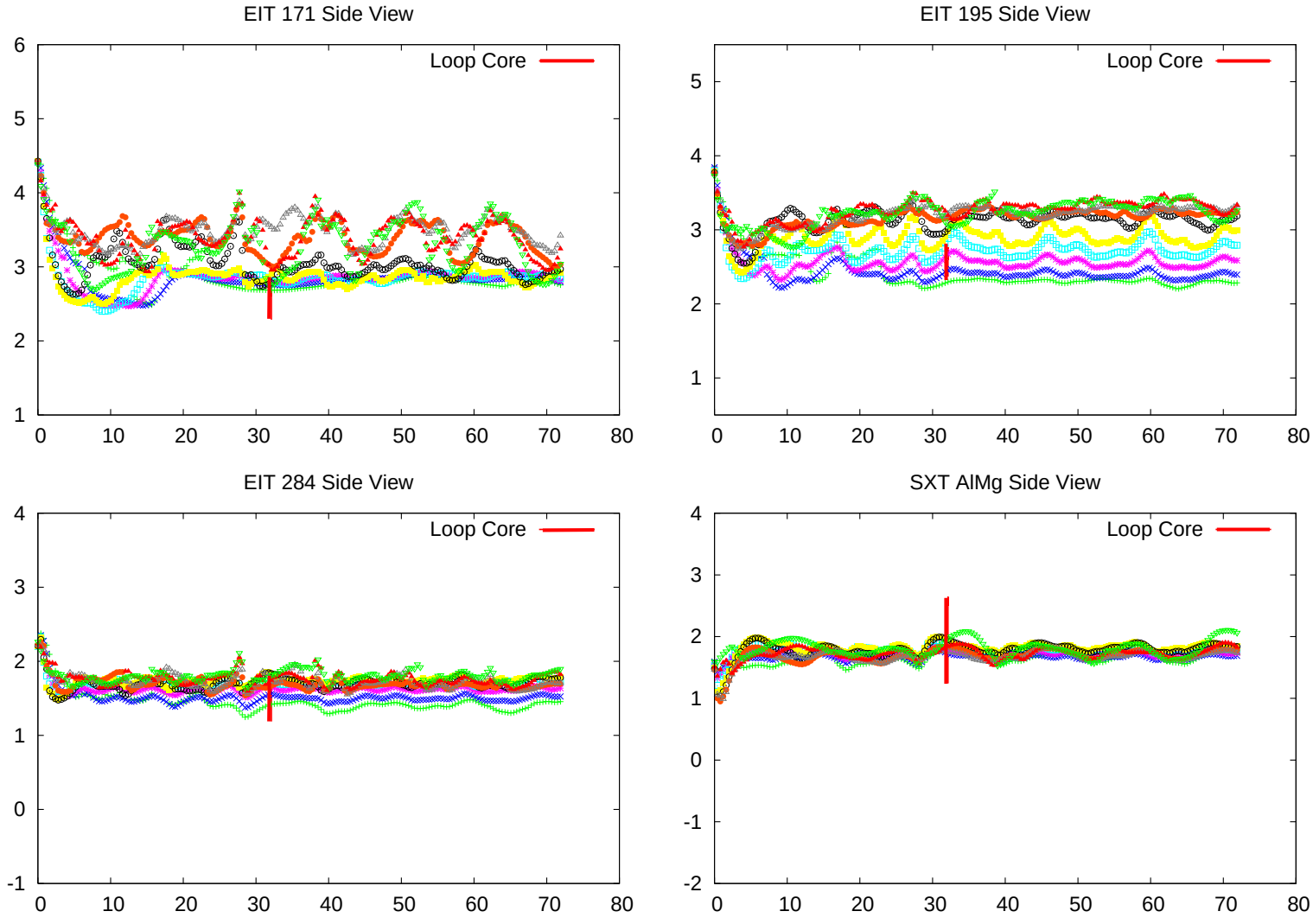

x axis: time in hours. y axis: emission in $\log 10\ DN/s/pixel$ (1024×1024 pixels).

Discussion

- The x axis shows time in hours. The y axis has emission in $\log 10\ DN/s/pixel$ for a resolution of 1024×1024 pixels.
- Cases with the same heating model have different constant of proportionality and/or different magnetic model (potential or sheared).
- Variations of the *average* emission, after the initial adjusting phase, are due to changes in the constant of proportionality.
- Thermal instabilities or non-equilibrium may cause non-steady emission.
- There are delays in the computed emission peaks in different bands.

Discussion (cont.)

- Calculated EUV emission in loop legs is too bright (a well known problem).
- Oscillations in emission from neighboring points are almost in phase. We have started to experiment using lower viscosity values in our simulations. We speculate that lowering viscosity would decouple the oscillations. Decoupling the emission oscillations in each strand would also make them invisible to the observer, who would only see the average emission composed by many strands.

Conclusions

- It is very difficult to match the emission in all bands and no model seems to reproduce perfectly the observed range of emission in all bands, although some models fare better than others.
- Comparing against different emission bands provides powerful physical constraints on parametric heating models of active regions.